

Reinhard Stösser  
 Gudrun Scholz  
 Jeannette Klein  
 Andrea Zehl  
 Werner Herrmann

## Spinresonance as a Bridge between Material- and Bioscience

The method of electron paramagnetic resonance (EPR) is based analogously to the nuclear magnetic resonance (NMR) on the interaction of electromagnetic radiation with magnetic moments, i.e. with electronic spin moments and electronic orbital moments interacting among each other, with nuclear moments and with external fields. Unpaired electrons yield in most cases a non-zero spin angular momentum, which can be used as a spectroscopic probe. Corresponding molecular systems are for instance free radicals, biradicals, triplet states, ions of transition metals and lanthanides. Beside the latter, point defects like trapped electrons and holes can be additionally observed in solids. Moreover, special structural and energetic situations allow the stabilization of atomic species such as  $H_s$ ,  $N_s$  or free radicals as already mentioned.

Subject of investigations by EPR are magnetic fields, resulting from internal and external contributions, at which the spins of the mentioned systems are in resonance with a monochromatic radiation ( $1 \text{ GHz} \leq \nu_{\text{mw}} \leq 100 \text{ GHz}$ ) [1]. Compared with NMR or optical spectroscopy the field of application of EPR is more limited, since unpaired electrons are relatively rare. This formal disadvantage, however, favours a selective examination of paramagnetic centres in a mainly diamagnetic environment. The genuine advantage of the EPR manifests in the specification for unpaired electrons in reactants, intermediates and products together with a high spectral resolution.

Unpaired spins can be detected in systems with completely different degree of order. They give information about the type, the strength and the time dependence of their interactions with the local magnetic fields in inorganic, organic and biologically relevant systems [1–6]. Therefore, information is accessible about very different states and events. Fig. 1 gives a schematic representation of EPR on non-crystalline solids and

\* Zero-field splitting stands for the splitting of the spin levels of probes with  $S \geq 1$  in the external field zero. This splitting depends directly on the symmetry of the local electric field. The spin coupling parameter  $b^0_2$  is a measure for the degree of distortion with axial symmetry. A further decrease of the symmetry has to be described with additional parameters like  $b^2_2$ ,  $b^0_4$ ,  $b^3_4$  [8]. Therefore, EPR spectra of spin probes with  $S \geq 1$  give unique information about details of the local electric field.

\*\* Based on the resonance condition  $h\nu = g\beta B_0$  the quantity  $g'$  defines the position in an EPR spectrum by

$$g' = \frac{h \cdot \nu}{\beta \cdot B}$$

i.e. the frequency/field ratio.

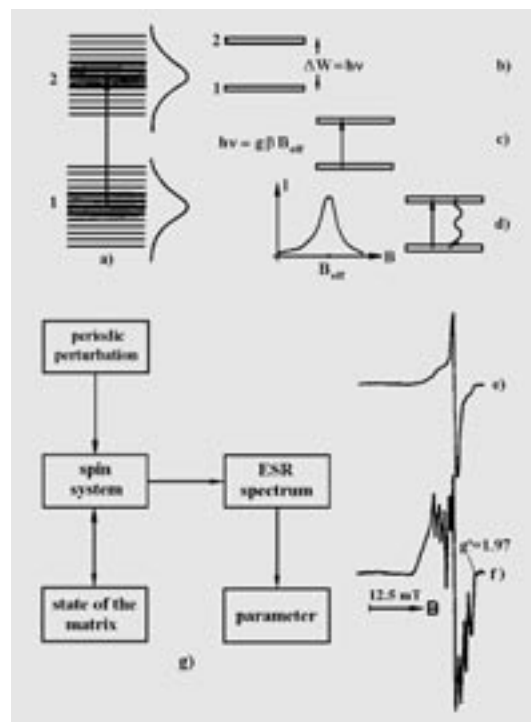


Fig. 1 Schematic representation of EPR on non-crystalline solids: a) transition between two (1 to 2) gaussian distributed sets of energy levels, b) to d) absorption of microwave quanta and relaxation, e), f) experimental EPR spectra of trapped holes in glassy (e) and crystalline (f) gehlenite, g) response of the spin system to periodic and matrix-induced perturbations.

displays the spectral difference of holes trapped in crystalline and non-crystalline phases of the same chemical composition [7].

### 1. In situ investigations of selected materials under the influence of mechanical forces and high temperatures

From a material science point of view it is of interest to combine the selectivity and sensitivity of the spectroscopic method EPR with macroscopic (ensemble) methods well established in material research. Such a direct combination can yield specific information which is not accessible by the individual methods alone.

Examples for the action of uniaxial pressure and for bending stress on glassy phase containing corundum samples are shown in Figs. 2 and 3. In both cases evidence is given for mechanically induced structural changes at a microscopic level. In principle, mechanical tensions can not be observed directly. Resulting deformations, however, are sensitively indicated and even transition-specifically detected by EPR. They will be quantitatively treated in (2) using statistical distributions of the zero-field splitting (zfs) parameters\* [1,8]. It has to be noted that the signal\*\* at  $g' \sim 4.3$ , representing  $Fe^{3+}$  ions in highly distorted coordination

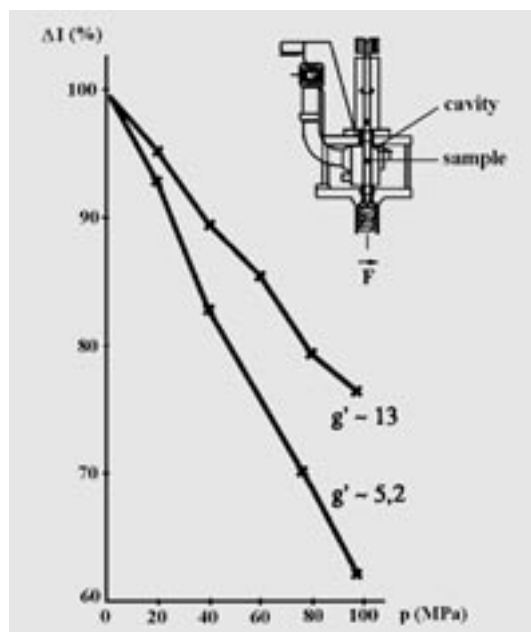


Fig. 2 Decrease of the intensities of  $Fe^{3+}$ -signals incorporated in a corundum material under the influence of a mechanical load in situ [8].

polyhedrons [7], yields only a small response to mechanical forces (s. Fig. 3a, b). Here, a direct correspondence exists to the effects of mechanical milling, e.g. to the production of nanostructured powders of  $\text{Al}_2\text{O}_3$  [9]. One of the advantages of *in situ* measurements is that structural relaxation processes, e.g. induced by periodic loading [10], can be directly observed. Such a procedure is common in material research and serves for a »mechanical training« of materials [11].

Beside the mechanical properties the thermal properties of a material are of great practical interest. On the one hand the thermal resistance and on the other hand the thermal activation of solids have to be characterized. One example in this field concerns the family of superhard materials indispensable in modern technologies. Natural and synthetic diamonds and their thermal and mechanical properties play a key role here. In Fig. 4 the EPR spectra of a powder of synthetic diamond are displayed. While the substitution of carbon atoms by  $^{14}\text{N}$  atoms ( $S=1/2$ ,  $I=1$ ) yields a spectrum with a typical anisotropic hyperfine structure (hfs) at room temperature (Fig. 4a), in the high-temperature state (1373 K *in situ*, Fig. 4b) a nearly isotropic hyperfine pattern of the  $^{14}\text{N}$  triplet results. At low temperature ( $\sim 300$  K) the hfs-anisotropy results from distortions of the »rigid« lattice of the diamond caused by the Jahn-Teller effect. Raising the temperature, the following effect is observable: in the range of  $\sim 500$  K the dynamic Jahn-Teller effect becomes active reducing continuously the distortion and yielding finally an isotropic  $^{14}\text{N}$ -hfs similar to that as commonly observed for NO-spin labels in fluid solu-

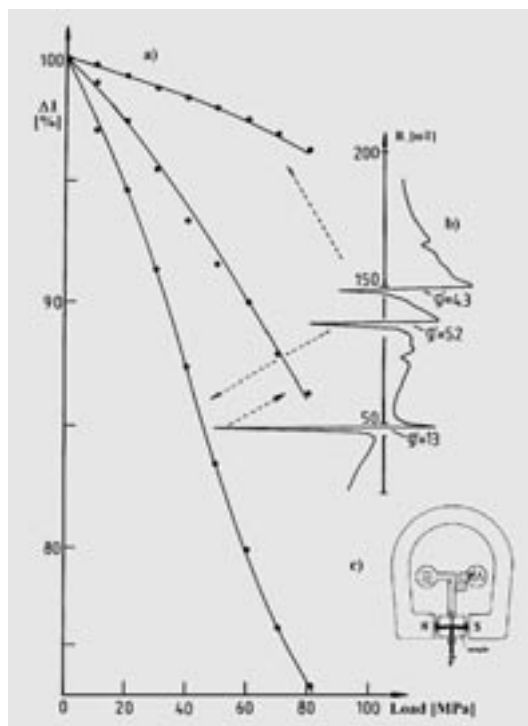


Fig. 3  
a) Decrease of the intensities of  $\text{Fe}^{3+}$  signals under influence of bending stress *in situ*,  
b) corresponding X band (9.3 GHz) EPR spectrum,  
c) schematic representation of the EPR apparatus used.

tions (s. 4). First attempts to simulate the spectra on the basis of the program developed by Freed et al. [12] yield reorientation-correlation times in the nanosecond range. Different charges of synthetic and natural diamonds exhibit different temperature effects on the spectral EPR response indicating interactions of the N atoms with paramagnetic and ferromagnetic impurities present as well as with lattice deformations. In combination with spin relaxation studies performed at

### Elektronenspinresonanz

Es wird eine kurze Einführung in das Phänomen der Elektronenspinresonanz (EPR) unter Hinweis auf aktuelle Entwicklungen in der Literatur gegeben. Anwendungen der EPR in der Materialforschung werden anhand von Beispielen zur *in situ*-Kombination der Methode mit mechanischen Methoden wie uniaxialer Druck und Biegebruch gegeben. Beispiele zur Hochtemperatur-EPR (max. 1400 K) beziehen sich auf den dynamischen Jahn-Teller Effekt von N-Atomen im Diamant sowie auf einen *in situ* Glasschmelzprozess.

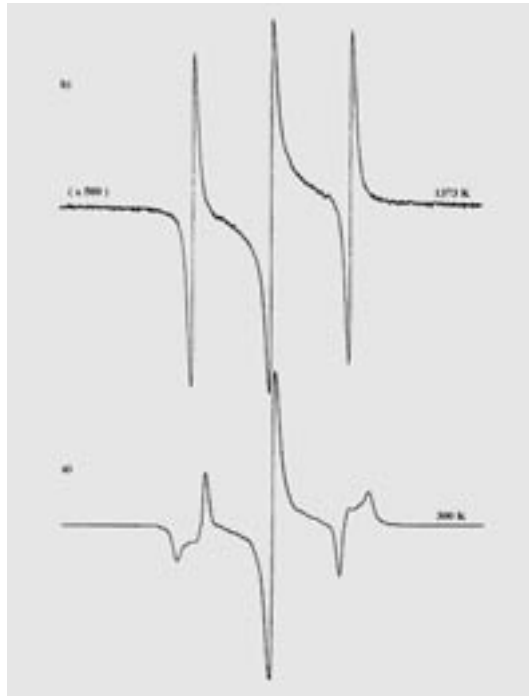
Probleme der quantitativen Interpretation der komplexen Multifrequenz-EPR Spektren von Spinsonden mit elektronischen S-Zuständen ( $\text{Fe}^{3+}$ ,  $\text{Mn}^{2+}$ ,  $\text{H}_2$ ) in Materialien mit koexistierenden kristallinen und

nicht-kristallinen Bereichen werden anhand fluoridischer und oxidischer Verbindungen des Al behandelt. Dabei wird der jeweils unterschiedliche Ordnungsgrad der Proben durch die Zahl und statistische Verteilung der den Spins zugänglichen energetischen Zustände explizit berücksichtigt.

Die methodische Brücke zwischen der Material- und Biowissenschaft wird exemplarisch hergestellt anhand des Superoxidanions  $\text{O}_2^-$ , stabilisiert in Strukturkäfigen eines Calciumaluminates. Die Bewegungszustände des  $\text{O}_2^-$  im Käfig werden mit Hilfe eines dynamischen Modells analysiert und die so gewonnenen Erkenntnisse auf die Spindynamik von NO-Spinsonden in Biosystemen übertragen. Mit Hilfe der EPR-Tomographie werden diese Prozesse in räumlich-spektraler Auflösung untersucht.

Fig. 4

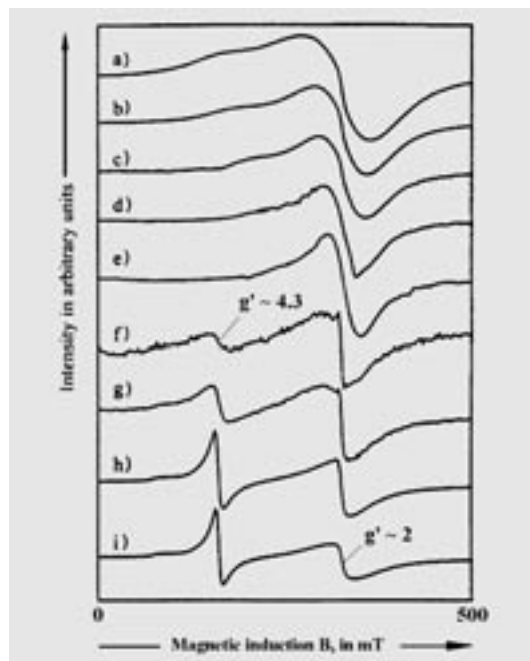
X band (9.3 GHz) EPR spectra of a synthetic diamond powder (AC20) ( $P_{mw}=20\mu W$ ) measured in situ  
a) at 300 K, and  
b) at 1373 K.



low temperatures valuable information can be extracted concerning the thermal and mechanical properties of the diamond samples. It should be noted that the number and coordination of the substituting  $^{14}N$  atoms are not only relevant for a spectroscopic indication but also for the enlargement of the brittle strength of the superhard material [11].

Fig. 5

Glass melting in the EPR spectrometer: series of EPR spectra of a batch of the composition (in mol%):  $60PbO-25B_2O_3-10ZnO-5SiO_2$ , + small amount of  $Fe_2O_3$  taken at:  
a) 296 K, b) 393 K, c) 493 K, d) 593 K, e) 693 K.  
After keeping the resulting melt at 873 K for 1 h it was stepwise cooled down to  
f) 803 K, g) 713 K, h) 448 K, i) 296 K.



A further example of high-temperature EPR concerns the watching of the process of inorganic glass melting inside the EPR cavity [7]. Fig. 5 collects the spectra starting from the batch for a low-melting glass. Up to 693 K the  $Fe^{3+}$  spin probes indicate by their spectral habit the formation of a glass, it means a distinct resonance in the low field appears. The resonance at  $g' \sim 4.3$  in Fig. 5f is comparatively broad. This reflects together with the intensive resonance at  $g' \sim 2$  an intermediate structural state of the molten mixture. Here only a part of the sample is transformed from the crystalline to the glassy state. The influence of the decreasing temperature (s. Fig. 5g to Fig. 5i) is manifested by a narrowing of the signal at  $g' \sim 4.3$  and a decreasing of the intensity at  $g' \sim 2$ . In dependence on the chemical composition of the glasses, the structural reorganization of the starting materials as well as the dynamics at a given temperature can be observed by high-temperature EPR. The latter leads to a change of the values of the zero-field splitting and their temperature dependent statistical distributions. (s. Fig. 1 and 3).

## 2. Spin probes in solids with coexisting crystalline and non-crystalline regions

A critical examination of the literature available reveals that in particular metastable phases, amorphous, as well as, nanostructured materials show desired specific properties necessary for their optimal use in material science. It is precisely the coexistence of regions and phases in solids with differing degrees of order, which is desirable in these fields.

Coexistence of crystalline and non-crystalline regions in fluoride and oxide aluminium compounds examined here appears in a quasi-stationary form in dehydration processes, during the application of mechanical impacts, and in processes of thermal annealing of glasses. For the oxide compounds they appear additionally at the annealing of sol-gel products. In combination with ensemble methods it can be proven by characteristic parameters of spin probes in electronic S-states.

Such a coexistence is realized in form of microcrystalline / nanocrystalline grains embedded in high distorted amorphous matrices. It can be understood as »discontinuous amorphous« state.

Derived from an actual entropy concept [13] the state of order of the matrix can be defined by the manifold of available energy states of the spin probes (s. Fig. 1) and manifests in typical, distinguishable EPR parameters of the probes localized in matrix parts with different degree of order. These are: (i) individual line

widths and line shapes, (ii) zero-field splitting parameters and the different extent of their distributions, and (iii) hyperfine and / or superhyperfine structures and their degrees of spectral resolution governed by broadening mechanisms of the individual hyperfine lines.

From a magnetic resonance point of view, the nature of coexistence of crystalline and non-crystalline regions yields different distribution widths of the spin-coupling parameters and their accompanying energy levels, respectively, for regions with different degrees of order. An increasing number of accessible energy levels consequently represents a lower degree of local order.

Broader distributions of available energy states in non-crystalline regions are due to irregular arrangements of coordination polyhedrons conserving their symmetries, distributions of distortions of the polyhedrons (distributions of bond distances  $R$  and bond angles  $\Theta$  and  $\Phi$ ), and the formation of dangling bonds as consequence of breaking bonds on external impacts.

Paramagnetic spin probes allow a selective, sensitive and simultaneous observation of coexisting crystalline and non-crystalline regions in fluoride and oxide aluminium powder matrices. Suitable spin probes for these purposes are atoms and ions with S-electronic ground states of different spin multiplicity, such as  $\text{Fe}^{3+}$ ,  $\text{Mn}^{2+}$  ( $S=5/2$ ) and atomic hydrogen  $H\alpha$  ( $S=1/2$ ) and examples will be given below.

For the first time, atomic hydrogen  $H\alpha$  could be stabilized at  $T \geq 293$  K in specially prepared fluoride and oxide compounds of aluminium:  $\{\text{AlF}_3\cdot\text{OH}\}$  and  $\{\text{AlOOH}_x\}$  [14,15]. The formation of atomic hydrogen was accomplished using different kinds of irradiation including  $\gamma$ -rays, X-rays and UV radiation, and even sunlight, these are those wavelengths in the region of  $\lambda \leq 254$  nm. A successful trapping of atomic hydrogen necessarily implies the coexistence of partial crystalline and amorphous regions in the powder samples (s. Fig. 6). For the formation and stabilization of atomic hydrogen in fluorides and oxides of aluminium following irradiation with different wave lengths and doses, each sample must meet three interrelated prerequisites: (i) symmetric host cages must be formed in a matrix capable of trapping  $H\alpha$ , (ii) crystalline and amorphous regions have to coexist in the sample, and (iii) an accessible amount of immobilized OH groups must be incorporated in the bulk of the materials to act as  $H\alpha$  precursors in the radiochemical as well as in the photochemical processes. In the aluminium flu-

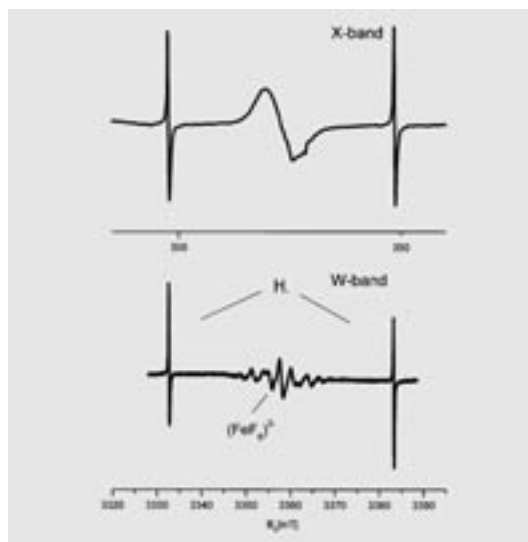
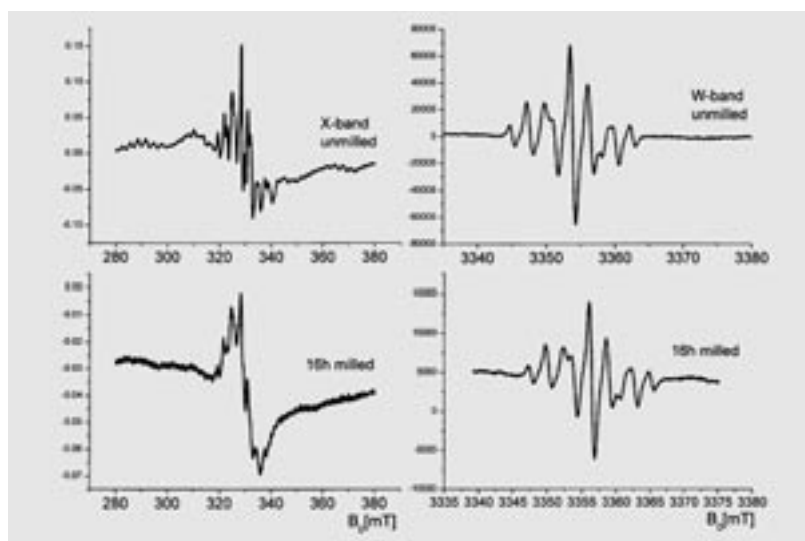


Fig. 6 X (9.3 GHz)- and W (94 GHz)-band EPR spectra following X irradiation for 10 h of a partial crystalline  $\text{AlF}_3$ -matrix (prepared from  $\beta$ - $\text{AlF}_3\cdot 3\text{H}_2\text{O}$ , annealed at 773 K for 1h).

oride and aluminium oxide samples mentioned above  $H\alpha$  acts as a spin probe in two ways: (i) that it can be trapped in cages and stabilized with Pauli repulsion indicates sensitively and unambiguously that there are local host nano-cages present in the matrices and, moreover, (ii) that it acts as a spin probe for determining the matrix state of order with its statistical distribution of coupling parameters, its spin dynamics as well as with the kinetic parameters of detrapping [14,15].

Whereas the  $H\alpha$ -trapping in the systems investigated is only possible in the case of coexisting crystalline and amorphous regions in a sample, the area of existence of the oxidation state of the transition metal ions  $\text{Fe}^{3+}$  and  $\text{Mn}^{2+}$  is much broader. Both ions can be

Fig. 7 X- and W-band EPR spectra (293 K) of unmilled  $\alpha$ - $\text{AlF}_3$  and an  $\text{AlF}_3$  sample milled for 16h in a planetary mill.





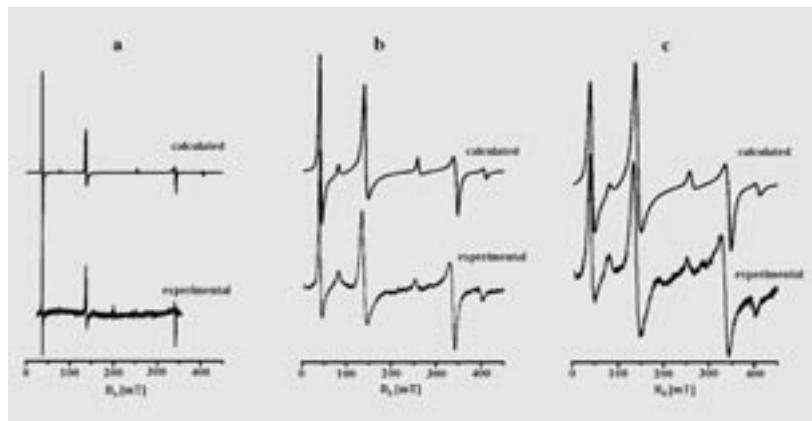
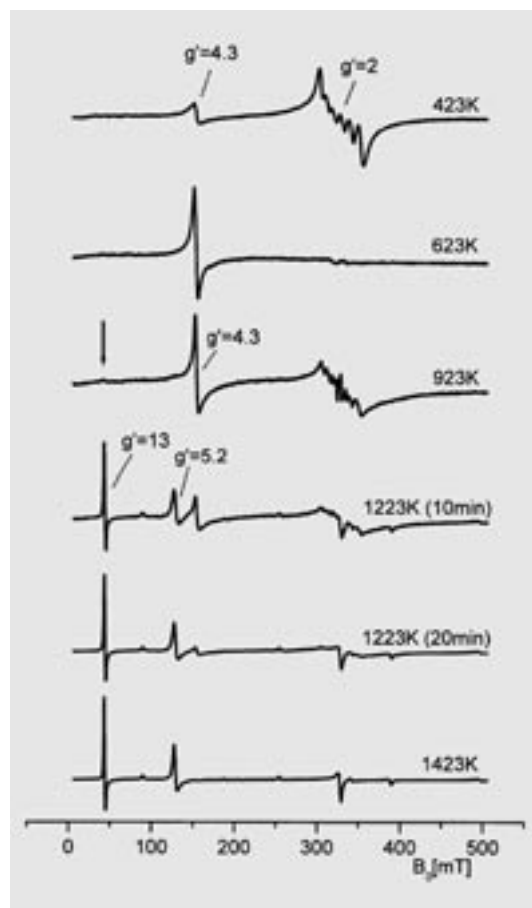


**Fig. 8**  
Experimental and calculated X-band EPR spectra of three different corundum samples: a) sample 1, b) sample 2, c) sample 3. (s. Table 1)

used to indicate and to characterize crystalline, partially crystalline as well as amorphous regions in a wide temperature range.

Multifrequency EPR spectra of  $\text{Fe}^{3+}$  ions in crystalline  $\alpha\text{-AlF}_3$  can be well reproduced using the zfs parameters given in Tab. 1. Due to the coupling with six equivalent fluorine nuclei the superhyperfine structure

**Fig. 9**  
X-band EPR spectra (293 K) for a thermally treated xerogel annealed for 30 min at the temperatures given in the figure, if not otherwise mentioned. An  $\alpha\text{-Al}_2\text{O}_3$  seeding was performed by adding an appropriate suspension to the sol.



can be resolved even in a matrix of crystalline  $\alpha\text{-AlF}_3$  powder. The latter implies that  $\text{Fe}^{3+}$  ions occupy cationic sites in the lattice.

In the fluoride matrices the different degree of matrix state of order can be mainly extracted from the degree of resolution of the superhyperfine structure (shfs) of  $(\text{FeF}_6)$  and  $(\text{MnF}_6)$  species in the  $g' \sim 2$  region of the EPR spectra. (s. Figs. 6, 7). That means, the resolution of the shfs in X band is governed by line broadening effects caused by interfering fine structure contributions. In X band the effect of fine structure contributions leads to a disappearance (Fig. 6) or bad resolution (Fig. 7, 16h milled sample) of the superhyperfine structure. The application of higher microwave frequencies (here W band, 94 GHz) gives additional information on still present highly ordered regions of the sample, indicated by a good resolution of the shfs. This is due to the neglecting influence of the zero-field splitting at such high fields (Figs. 6, 7).

In the case of »continuous« amorphous fluoride samples, like glasses, the distribution of bond lengths and bond angles and therewith of zfs parameters of the  $d^5$ -ions is responsible for additional resonance transitions at the effective g-value of  $g' \sim 4.3$  beside the broad resonance at  $g' \sim 2$  in X-band [8,16].

In aluminium oxide matrices the local order is dominantly reflected by the zfs parameters of the  $\text{Fe}^{3+}$  ions and their statistical distributions. Beside the three zfs parameters (s. Table 1), which correspond to the symmetry of the local crystalline field, a small distribution of an additional zfs parameter,  $\delta b_2^2$  has to be taken into account. The latter implies a decrease of the local site symmetry for  $\text{Fe}^{3+}$  ions already in nominally unperturbed corundum samples (s. Fig. 8, Table 1). It could be shown that the distribution width of this zfs parameter ( $b_2^2$ ) can be regarded as a precise measure of the crystalline quality of various corundum samples, an effect which at this order of magnitude can only hardly be seen by conventional XRD measurements (s. Fig. 3) [9, 17]. Corundum samples with different iron contents require different distributions widths  $\delta b_2^2$  (s. Fig. 8). It means that  $\text{Fe}^{3+}$  ions in corundum matrices do not fully accept their local symmetry, which might have consequences for their behaviour as spin probes for local chemical reactions and/or for reactions of the bulk as a whole.

One example, were the character of  $\text{Fe}^{3+}$  ions as spin probes and reaction centres implies in fact no discrepancy in oxide materials, is the corundum formation using the sol-gel preparation route. It is well known

that  $\text{Fe}^{3+}$  ions interfere with the process of corundum formation on the sol-gel route by distinctly decreasing the crystallization temperature, a process which is desired [18]. On the other hand their characteristic X band EPR signals at  $g' \sim 13$  and  $g' \sim 5.2$  sensitively indicate the local corundum formation in the matrices. At low concentrations,  $\text{Fe}^{3+}$  ions give information on coexisting local crystalline ( $g' \sim 13$  and  $g' \sim 5.2$ ) and amorphous regions ( $g' \sim 4.3$ ), due to their distinctly separated signals (s. Fig. 9). (Tab. 1)

### 3. Trapped electrons, holes, small molecules and organic radicals stabilized in inorganic solids

Electrons and holes can be generated and trapped after energetic impacts endured on crystalline and/or non-crystalline solids. Such electronic defects could be traced in many terrestrial and even lunar materials [19, 20]. In general they originate from the interaction of high-energy irradiation (e.g.  $\gamma$ -irradiation) with the material and can be used to draw conclusions concerning the structure and the age [20, 21] of the samples.

From a material science point of view the characterization of glasses [7] and ceramics can be done with respect to the changing properties of the materials, like transparency or refractive indices, under the influence of high-energetic impacts (e.g. Laser irradiation [22]).

Concerning organic radicals, which could be observed in inorganic matrices, an essential precondition is the existence or thermally induced formation of suitable cavities (see also 3., trapping of  $H_2$  atoms). The latter should allow both the stabilization and the study of such types of radicals by stationary methods. That avoids the difficulties due to their short live times. Different short living C-, Si- and O-centred radicals could be produced and identified in this way [23].

One paramagnetic species is of special interest in connection with problems treated in this paper. It is the formation and stabilization of the superoxide anion  $O_2^-$  in the material  $12 \text{ CaO} \cdot 7 \text{ Al}_2\text{O}_3$  ( $\text{C}_{12}\text{A}_7$ ) [24]. This material represents an essential component of cement because of its hydraulic properties. The  $O_2^-$  ion is generated by the thermal energy at the formation of the phase  $\text{C}_{12}\text{A}_7$  at 1473 K and stabilized in structural cavities. The latter were evidenced by XRD [24]. The importance of the discovery of this species is not restricted to material science. On the contrary, it yields an excellent model system for catalytic and biomedical research. Even in such research this paramagnetic species is often postulated or only indirectly prov-

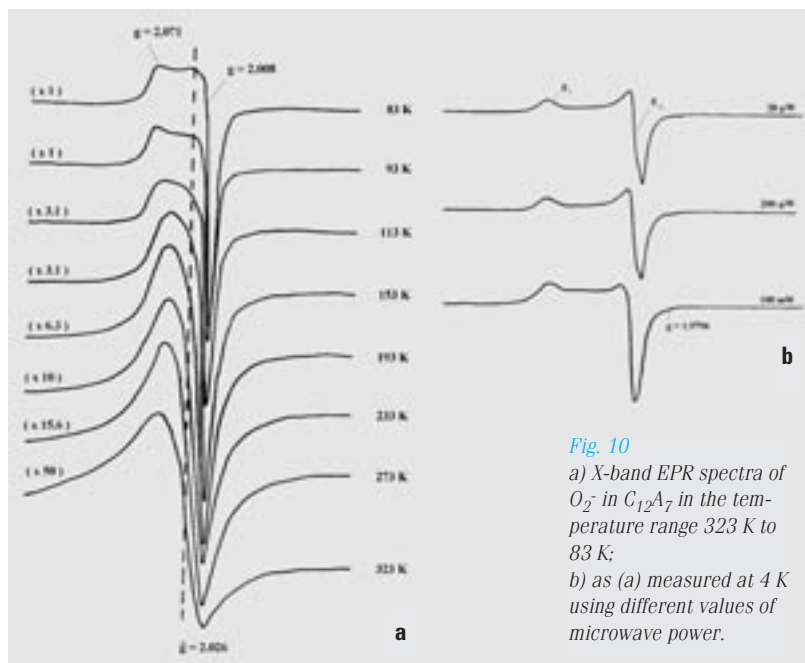


Fig. 10  
a) X-band EPR spectra of  $O_2^-$  in  $\text{C}_{12}\text{A}_7$  in the temperature range 323 K to 83 K;  
b) as (a) measured at 4 K using different values of microwave power.

en. The EPR spectra are often of low quality because of the small stationary concentrations of the reactive species. In dependence on the partial pressure of oxygen present at the synthesis of the calciumaluminate a large  $O_2^-$  concentration can be reached and EPR spectra of good quality are observable. There is a remarkable long-time stability of the trapped species lasting

Tab. 1

<b>Zero-field splitting (zfs) parameters of <math>\text{Fe}^{3+}</math> ions in <math>\alpha\text{-AlF}_3</math> and <math>\alpha\text{-Al}_2\text{O}_3</math> powders as determined by calculation [9, 17] (in <math>10^{-4} \text{ cm}^{-1}</math>)</b>				
matrix	$b_2^0$	$b_4^0$	$b_4^3$	$\delta b_2^2$
$\alpha\text{-AlF}_3$	167	-15	425	–
$\alpha\text{-Al}_2\text{O}_3$				
sample 1	1705	-108	2181	$25 \pm 5$
sample 2				$80 \pm 10$
sample 3				$80 \pm 10$

sample 1: 0.0002 mol%  $\text{Fe}_2\text{O}_3$ ; sample 2: 0.26 mol%  $\text{Fe}_2\text{O}_3$ ; sample 3: 1.04 mol%  $\text{Fe}_2\text{O}_3$ .

over years. Fig. 10a depicts the EPR spectra of  $O_2^-$  in  $\text{C}_{12}\text{A}_7$  at different temperatures. It becomes evident that the isotropic spectrum recorded at 323 K results from the anisotropic one observable at 4 K (Fig. 10b) by motional effects of the molecule in the structural cavity of  $\text{C}_{12}\text{A}_7$ .

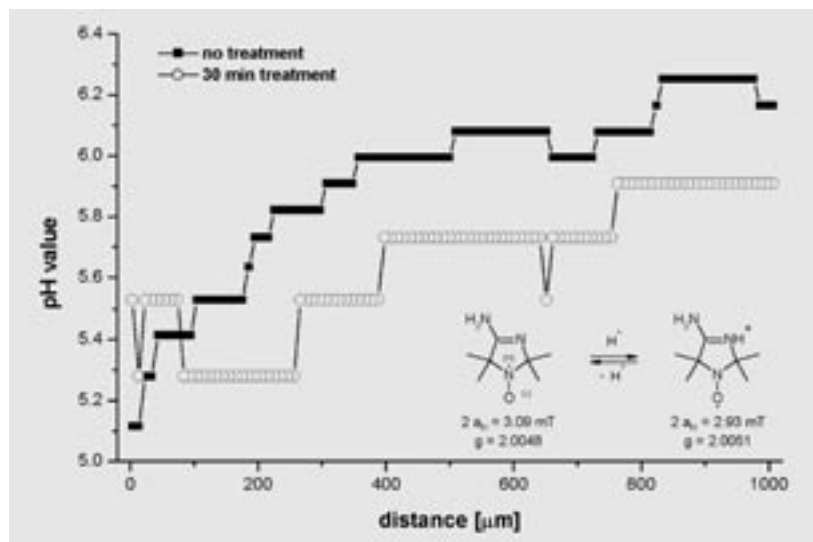


**Fig. 11**  
Spatial pH profile inside a human skin sample as result of the treatment with salicylic acid. The pH profile was determined with the acid-base equilibrium of the spin probes shown in the inset.

Furthermore, at 4 K the increase of microwave power in the EPR experiment results in a deformation of the spectral habit in the range between  $g_{||}$  and  $g_{\perp}$  (Fig. 10b), indicating the activation of the  $O_2^-$  movements caused by the small amount of thermal energy brought into the system via microwave radiation. Simulations based on a dynamic model developed by Freed [12] lead to the following statements: The reorientation of the  $O_2^-$  molecule is thermally activated and starts even at very low temperatures. Based on this model the unexpected spectral effects observed by EPR on

treatment at 1223 K in an  $O_2$  atmosphere, the signal disappears in a  $N_2/H_2$  (9:1) atmosphere [26].

#### 4. EPR studies of biologically relevant systems

A manifold of new applications of EPR can be observed in the field of biosciences. This concerns methodical developments [27] as well as completely new applications to rather different biologically relevant objects. Although there is a particularly significant progress in the application of pulse and high-field techniques [3, 5], now the interest will be focused on the penetration and permeation processes of spin probes in biological objects (like human skin)\*\*\* reporting about the polarity and pH values (s. Fig. 11) in the environment of their probes and on their movement regime in spatially separated layers of a sample or animal. For this purpose EPR spectra were recorded with spectral and spatial resolution by means of EPR tomography [28, 29]. The obtained spectra after image reconstruction were discussed by means of models used for the simulation of the spectra of N-atoms in diamond (see 1) and  $O_2^-$  in  $C_{12}A_7$  (see 4.) yielding the  $\tilde{g}$  and  $\hat{A}$ -coupling matrices together with the time constants  $\tau_R$  of the reorientation correlation in every layer of the object.

#### Acknowledgement

The authors kindly acknowledge Dr. M. Nofz (BAM Berlin), Dr. M. Päch (Humboldt-Universität zu Berlin), Prof. Dr. J. Y. Buzaré and Dr. G. Silly (Université du Maine, France), Prof. Dr. H. H. Borchert, K. P. Moll (Freie Universität Berlin), Prof. Dr. K. Mäder (Martin-Luther-Universität Halle), Dr. F. Lenzian (Technische Universität Berlin) and Dr. E. Janata (HMI Berlin) for their fruitful cooperation and support.

#### References

- [1] J. A. Weil / J. R. Bolton / J. E. Wertz: Electron Paramagnetic Resonance, J. Wiley & Sons New York, 1994.
- [2] L. Kevan / M. K. Bowman: Modern pulsed and continuous-wave electron spin resonance, J. Wiley & Sons New York, 1990.
- [3] A. Schweiger / G. Jeschke: Principles of Pulse Electron Paramagnetic Resonance, Oxford University Press, 2001.
- [4] H. Kurreck, / B. Kirste / W. Lubitz: Electron nuclear double resonance spectroscopy of radicals in solution: application to organic and biological chemistry, VCH Weinheim, 1988.
- [5] K. Möbius, Chem. Soc. Rev. 29 (2000) 129–139. Primary processes in photosynthesis: what do we learn from high-field EPR spectroscopy?.
- [6] M. Mehring / V.A. Weberruß: Object-oriented magnetic resonance, Academic Press, San Diego, New York, 2001.

**Tab. 2**

**Calculated time constants  $\tau_R$  [s] for reorientation of  $O_2^-$  in  $C_{12}A_7$  at different temperatures<sup>(1)</sup>**

T[K]	$\tau_R$ (I)	$\tau_R$ (II)
323	$1.3 \cdot 10^{-9}$ (100%)	
153	$5.8 \cdot 10^{-9}$ (55%)	$3.2 \cdot 10^{-8}$ (45%)
83	$6.1 \cdot 10^{-9}$ (44%)	$4.6 \cdot 10^{-8}$ (56%)

<sup>(1)</sup> The application of the dynamic model for simulation is based on the assumption of the coexistence of two  $O_2^-$  species in different states of movement (I, II).

electrochemically generated  $O_2^-$  in butyronitrile up to 222 K can be elucidated [25]. The reorientation is in part active even at 4 K. The time constants for the reorientations are given in Table 2. The values allow the estimation of the activation energies of the process. (Tab. 2)

Whereas the EPR amplitude and therefore the number of  $O_2^-$  spins can be significantly enhanced by thermal

\*\*\* All these studies were performed in the group of Prof. Dr. H. H. Borchert (Humboldt-Universität zu Berlin/Freie Universität Berlin, Dept. of Pharmacy).

- [7] R. Stösser / M. Nofz, *Glastech. Ber. Glass Sci. Technol.* 67 (1994) 156–170. ESR spectroscopy on glasses and glassy-crystalline materials – new opportunities for material scientists.
- [8] G. Scholz / R. Stösser / M. Krossner / J. Klein, *Appl. Magn. Res.* 21 (2001) 105–123. Modelling of multifrequency ESR spectra of Fe<sup>3+</sup> ions in crystalline and amorphous materials: a simplified approach to determine statistical distributions of spin-spin coupling parameters.
- [9] G. Scholz / R. Stösser / J. Klein / G. Silly / J. Y. Buzaré / Y. Lalgant / B. Ziemer, *J. Phys.: Condens. Matter* 14 (2002) 2101–2117. Local structural orders in nanostructured Al<sub>2</sub>O<sub>3</sub> prepared by high-energy ball milling.
- [10] R. Stösser / R. Brenneis, *High Pressure Research* 13 (1994) 71–75. In situ measurement of pressure and strain effects in corund ceramics.
- [11] R. Stösser / A. Rericha / B. Pritze, *High Press. Res.* 7 (1991) 192–194. Peculiarities of magnetic properties induced by mechanical impacts at the manufacturing of diamond micron powders.
- [12] D. E. Budil / S. Lee / S. Saxena / J. H. Freed, *J. Magn. Res. A* 120 (1996) 155–189. Nonlinear-least squares analysis of slow-motion EPR spectra in one and two dimensions using a modified Levenberg-Marquardt algorithm.
- [13] F. L. Lambert, *J. Chem. Ed.* 79(2) (2002) 187–192. Disorder – a cracked crutch for supporting entropy discussions.
- [14] G. Scholz / R. Stösser, *Phys. Chem. Chem. Phys.* 4 (2002) 5448–5457. Atomic hydrogen as spin probe in thermally and mechanically activated materials.
- [15] G. Scholz / R. Stösser / J. A. Momand / A. Zehl / J. Klein, *Angew. Chemie*, 112(14) (2000) 2570; *Angew. Chemie, Int. Ed.* 39(14) (2000) 2516–2519. Aluminium fluoride as a storage matrix für atomic hydrogen.
- [16] R. Stösser / G. Scholz, *Appl. Magn. Res.* 12 (1997) 167–181. ESR evidence of order/disorder transitions in solids caused by dehydration.
- [17] Y. Buzaré, / G. Silly / J. Klein / G. Scholz / R. Stösser / M. Nofz, *J. Phys.: Condens. Matter* 14 (2002) 10331–10348. Electron paramagnetic resonance investigations of  $\alpha$ -Al<sub>2</sub>O<sub>3</sub> powders doped with Fe<sup>3+</sup> ions: experiments and simulations.
- [18] M. Nofz / R. Stösser / G. Scholz, (2003) in preparation. Thermal and spectroscopic indication of early stages of corundum formation in seeded and Fe<sup>3+</sup> doped boehmite gels.
- [19] J. Non-Crystalline Solids, 179 (1994). The R. A. Weeks International Symposium on Science and Technology of SiO<sub>2</sub> and Related Materials, Eds.: D. L. Griscom and H. Hosono, Elsevier Science B. V. 1994.
- [20] R. Stösser / J. Bartoll / L. Schirrmeister / R. Ernst / R. Lück, *Appl. Rad. Isotop.* 47 (1996) 1489–1499. ESR of trapped holes and electrons in natural and synthetic carbonates and aluminosilicates.
- [21] M. Ikeya, *New applications of Electron Spin Resonance – dating, dosimetry and microscopy*, World Scientific, Singapore 1993.
- [22] R. Stösser / M. Nofz, *Phys. Chem. Glasses* 42 (2001) 401–407. Generation and stimulated decay of paramagnetic centres in laser excited glasses.
- [23] R. Stösser / M. Päch, *Appl. Radiat. Isotopes* 55 (2001) 215–220. Contributions to the radiation chemistry of octasilsesquioxanes: unique traps für atomic hydrogen and free radicals at ambient temperature.
- [24] R. Stösser / M. Nofz / W. Gessner / Ch. Schröter / G. Kranz, *J. Solid State Chem.* 81 (1989) 152–164. Paramagnetic monitors (Mn<sup>2+</sup>, Mn<sup>4+</sup>, Fe<sup>3+</sup>, O<sub>2</sub>) in the solid state reaction yielding 12 CaO.7 Al<sub>2</sub>O<sub>3</sub> and other aluminates.
- [25] R. N. Bagchi / A. M. Bond / F. Scholz / R. Stösser, *J. Am. Chem. Soc.* 111 (1989) 8270–8271. Characterization of the ESR spectrum of the superoxide anion in the liquid phase.
- [26] R. Stösser / W. Herrmann / M. Nofz / M. Päch, (2003) in preparation.
- [27] J. H. Freed, *Ann. Rev. Phys. Chem.* 51 (2000) 655–689. New technologies in Electron Spin Resonance.
- [28] K. Mäder / S. Nitschke / R. Stösser / H.-H. Borchert / A. Domb, *Polymer* 38 (19) (1997) 4785–4794. Non-destructive and localized assessment of acidic microenvironments inside biodegradable polyanhydrides by spectral spatial electron paramagnetic resonance imaging.
- [29] C. Kroll / W. Herrmann / R. Stösser / H. H. Borchert / K. Mäder, *Pharmac. Res.* 18 (2001) 525–530. Influence of drug treatment on the microacidity in rat and human skin – an in vitro electron spin resonance imaging study.



**Prof. Dr. rer. nat.  
Reinhard Stösser**

Born 1939. 1965 diploma in Chemistry at the Humboldt-Universität zu Berlin; since 1992 head of the research group ESR-spectroscopy at the Institute of Physical and Theoretical Chemistry (Humboldt-Universität); 1993 Professor of Physical and Theoretical Chemistry at the Humboldt-Universität zu Berlin.

Research interests: Development and application of ESR spectroscopy in the field of solid state chemistry in relation to catalysis, material science as well as biological sciences (ESR investigations at 2 – 95 GHz in the temperature range 2.5 K  $\leq$  T  $\leq$  1450 K (X-band)); Examination of spectral and spatial distributions of nitroxyl radicals and model pharmaca in vitro and in-vivo.

#### Contact

Humboldt-Universität  
zu Berlin  
Faculty of Mathematics  
and Natural Sciences I  
Department of Chemistry  
Brook-Taylor-Str. 2  
D-12489 Berlin-Adlershof  
Phone: +49 30 2093-7108  
Fax: +49 30 2093-7110  
E-Mail:  
reinhard.stoesser@  
rz.hu-berlin.de  
www.chemie.hu-berlin.de/  
stoesser/index.html